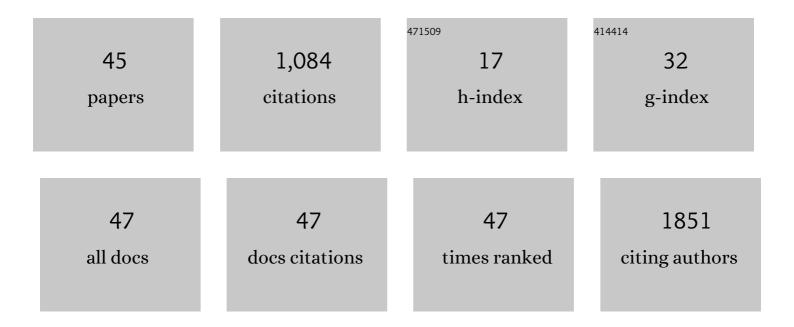
Richard Southworth

List of Publications by Year in descending order

Source: https://exaly.com/author-pdf/6178362/publications.pdf Version: 2024-02-01



#	Article	IF	CITATIONS
1	Detecting Validated Intracellular ROS Generation with 18F-dihydroethidine-Based PET. Molecular Imaging and Biology, 2022, 24, 377-383.	2.6	4
2	A Reactivity-Based ¹⁸ F-Labeled Probe for PET Imaging of Oxidative Stress in Chemotherapy-Induced Cardiotoxicity. Molecular Pharmaceutics, 2022, 19, 18-25.	4.6	2
3	Synthesis and <i>ex vivo</i> biological evaluation of gallium-68 labelled NODAGA chelates assessing cardiac uptake and retention. Dalton Transactions, 2021, 50, 14695-14705.	3.3	2
4	Gallium: New developments and applications in radiopharmaceutics. Advances in Inorganic Chemistry, 2021, 78, 1-35.	1.0	9
5	DO2A-based ligands for gallium-68 chelation: synthesis, radiochemistry and <i>ex vivo</i> cardiac uptake. Dalton Transactions, 2020, 49, 1097-1106.	3.3	12
6	Detection of anthracycline-induced cardiotoxicity using perfusion-corrected 99mTc sestamibi SPECT. Scientific Reports, 2019, 9, 216.	3.3	18
7	Imaging of Chemotherapy-Induced Acute Cardiotoxicity with ¹⁸ F-Labeled Lipophilic Cations. Journal of Nuclear Medicine, 2019, 60, 1750-1756.	5.0	26
8	Tissue acidosis does not mediate the hypoxia selectivity of [64Cu][Cu(ATSM)] in the isolated perfused rat heart. Scientific Reports, 2019, 9, 499.	3.3	6
9	PET Imaging of Cardiac Hypoxia: Hitting Hypoxia Where It Hurts. Current Cardiovascular Imaging Reports, 2018, 11, 7.	0.6	12
10	Synthesis, gallium-68 radiolabelling and biological evaluation of a series of triarylphosphonium-functionalized DO3A chelators. Dalton Transactions, 2018, 47, 15448-15457.	3.3	10
11	Modeling nonâ€linear kinetics of hyperpolarized [1â€ ¹³ C] pyruvate in the crystalloidâ€perfused rat heart. NMR in Biomedicine, 2016, 29, 377-386.	2.8	17
12	Opportunities and Challenges for Metal Chemistry in Molecular Imaging. Advances in Inorganic Chemistry, 2016, 68, 1-41.	1.0	12
13	Kinetic analysis of hyperpolarized data with minimum a priori knowledge: Hybrid maximum entropy and nonlinear least squares method (MEM/NLS). Magnetic Resonance in Medicine, 2015, 73, 2332-2342.	3.0	5
14	Multiple quantum filtered 23Na NMR in the Langendorff perfused mouse heart: Ratio of triple/double quantum filtered signals correlates with [Na]i. Journal of Molecular and Cellular Cardiology, 2015, 86, 95-101.	1.9	22
15	64Cu-CTS: A Promising Radiopharmaceutical for the Identification of Low-Grade Cardiac Hypoxia by PET. Journal of Nuclear Medicine, 2015, 56, 921-926.	5.0	24
16	Cardiac Hypoxia Imaging: Second-Generation Analogues of ⁶⁴ Cu-ATSM. Journal of Nuclear Medicine, 2014, 55, 488-494.	5.0	37
17	Targeting hexokinase <scp>II</scp> to mitochondria to modulate energy metabolism and reduce ischaemiaâ€reperfusion injury in heart. British Journal of Pharmacology, 2014, 171, 2067-2079.	5.4	91
18	Modification of intracellular glutathione status does not change the cardiac trapping of 64Cu(ATSM). EJNMMI Research, 2014, 4, 40.	2.5	10

RICHARD SOUTHWORTH

#	Article	IF	CITATIONS
19	Assessing radiotracer kinetics in the Langendorff perfused heart. EJNMMI Research, 2013, 3, 74.	2.5	11
20	Pathophysiological Consequences of TAT-HKII Peptide Administration Are Independent of Impaired Vascular Function and Ensuing Ischemia. Circulation Research, 2013, 112, e8-13.	4.5	11
21	Demonstration of the retention of 64Cu-ATSM in cardiac myocytes using a novel incubation chamber for screening hypoxia-dependent radiotracers. Nuclear Medicine Communications, 2013, 34, 1015-1022.	1.1	11
22	Trapped Platelets Activated in Ischemia Initiate Ventricular Fibrillation. Circulation: Arrhythmia and Electrophysiology, 2013, 6, 995-1001.	4.8	11
23	Developing Hyperpolarized 13C Spectroscopy and Imaging for Metabolic Studies in the Isolated Perfused Rat Heart. Applied Magnetic Resonance, 2012, 43, 275-288.	1.2	9
24	PET imaging of cardiac hypoxia: Opportunities and challenges. Journal of Molecular and Cellular Cardiology, 2011, 51, 640-650.	1.9	41
25	08 Disruption of hexokinase II-mitochondrial binding affects cardiac oxygen consumption and lactate production in the beating heart. Heart, 2011, 97, e8-e8.	2.9	0
26	Disruption of Hexokinase II–Mitochondrial Binding Blocks Ischemic Preconditioning and Causes Rapid Cardiac Necrosis. Circulation Research, 2011, 108, 1165-1169.	4.5	73
27	07 Mitochondrial hexokinase II is essential for cardiac function and ischaemic preconditioning. Heart, 2011, 97, e8-e8.	2.9	0
28	Monitoring of In Vivo Function of Superparamagnetic Iron Oxide Labelled Murine Dendritic Cells during Anti-Tumour Vaccination. PLoS ONE, 2011, 6, e19662.	2.5	42
29	An isolated perfused pig heart model for the development, validation and translation of novel cardiovascular magnetic resonance techniques. Journal of Cardiovascular Magnetic Resonance, 2010, 12, 53.	3.3	43
30	Renal vascular inflammation induced by Western diet in ApoE-null mice quantified by 19F NMR of VCAM-1 targeted nanobeacons. Nanomedicine: Nanotechnology, Biology, and Medicine, 2009, 5, 359-367.	3.3	57
31	Hexokinase-mitochondrial interaction in cardiac tissue: implications for cardiac glucose uptake, the 18FDG lumped constant and cardiac protection. Journal of Bioenergetics and Biomembranes, 2009, 41, 187-193.	2.3	15
32	Immunogold labeling study of the distribution of GLUT-1 and GLUT-4 in cardiac tissue following stimulation by insulin or ischemia. American Journal of Physiology - Heart and Circulatory Physiology, 2007, 292, H2009-H2019.	3.2	39
33	A reevaluation of the roles of hexokinase I and II in the heart. American Journal of Physiology - Heart and Circulatory Physiology, 2007, 292, H378-H386.	3.2	53
34	Mitochondrial uncoupling, with low concentration FCCP, induces ROS-dependent cardioprotection independent of KATP channel activation. Cardiovascular Research, 2006, 72, 313-321.	3.8	205
35	The low oxygen-carrying capacity of Krebs buffer causes a doubling in ventricular wall thickness in the isolated heart. Canadian Journal of Physiology and Pharmacology, 2005, 83, 174-182.	1.4	7
36	Tissue-specific differences in 2-fluoro-2-deoxyglucose metabolism beyond FDG-6-P: a19F NMR spectroscopy study in the rat. NMR in Biomedicine, 2003, 16, 494-502.	2.8	51

#	Article	IF	CITATIONS
37	Dobutamine responsiveness, PET mismatch, and lack of necrosis in low-flow ischemia: is this hibernation in the isolated rat heart?. American Journal of Physiology - Heart and Circulatory Physiology, 2003, 285, H316-H324.	3.2	15
38	18FDG6P and 14C DG6P accumulation differ in the isolated heart: An autoradiographic study. Journal of Molecular and Cellular Cardiology, 2002, 34, A59.	1.9	0
39	An isolated rat heart model of acute hibernation confirmed by flow-metabolism "mis-match―(PET) & dobutamine response. Journal of Molecular and Cellular Cardiology, 2002, 34, A60.	1.9	0
40	Lactate-induced translocation of GLUT1 and GLUT4 is not mediated by the phosphatidylinositol-3-kinase pathway in the rat heart. Basic Research in Cardiology, 2002, 97, 168-176.	5.9	21
41	Dissociation of glucose tracer uptake and glucose transporter distribution in the regionally ischaemic isolated rat heart: application of a new autoradiographic technique. European Journal of Nuclear Medicine and Molecular Imaging, 2002, 29, 1334-1341.	6.4	16
42	Lactate translocates GLUT4 and GLUT1 but decreases the accumulation of 2-deoxy-D-glucose-6P (DG6P) in the rat heart. Journal of Molecular and Cellular Cardiology, 2001, 33, A172.	1.9	0
43	Ischaemia and reperfusion increase sarcolemmal GLUT4 but decrease 2-fluoro-2-deoxyglucose-6P (FDGCP) accumulation. Journal of Molecular and Cellular Cardiology, 2001, 33, A176.	1.9	1
44	Differential uptake of FDG and DG during post-ischaemic reperfusion in the isolated, perfused rat heart. European Journal of Nuclear Medicine and Molecular Imaging, 1999, 26, 1353.	2.1	19
45	Developmental Differences in Superoxide Production in Isolated Guinea-Pig Hearts During Reperfusion. Journal of Molecular and Cellular Cardiology, 1998, 30, 1391-1399.	1.9	13